Supporting Information

Oakhill et al. 10.1073/pnas.1009705107

SI Methods and Materials

Protein Production. Details of expression plasmids used are provided in Table S1. All mutants were generated using Quikchange site-directed mutagenesis kits (Stratagene) and all constructs were sequence verified. AMP-activated protein kinase (AMPK) expressed in COS7 (GST-α1/2, β1/2, HA-γ1) or Sf21 insect cells (GST-α1β1γ1), and FLAG-CaMKKβ expressed in Sf21 cells were purified as described previously (1, 2). Briefly, AMPK from COS7 cells was purified using glutathione Sepharose 4B (GE Life Sciences). AMPK and PP2c from Sf21 cells were purified using a combination of glutathione Sepharose, anion-exchange (Q-Sepharose, GE Life Sciences) and size exclusion chromatography (Superdex-200, GE Life Sciences). GST tag was completely removed from PP2c by Tobacco Etch Virus protease treatment prior to the ion-exchange step. AMPK [maltose binding protein (MBP)-α1β1γ1] was expressed in *Escherichia coli* (0.25 mM IPTG induction, 4 h, 32 °C) and purified using amylose agarose (NEB) followed by size exclusion chromatography. Myristoylated AMPK was expressed in *E. coli* cotransformed with MBP-AMPK and N-myristoyl transferase (3) (a generous gift from Prof. Jeffrey Gordon, Washington University, St. Louis). Octyl glucopyranoside (0.1% wt/vol) was included in all buffers during purification and aggregated myristoylated AMPK was removed by size exclusion chromatography. For each AMPK expression system, the presence of heterotrimeric AMPK was confirmed by TOF mass spectrometry. Sf21 or COS7 cell-expressed AMPK bound to 100 μL glutathione Sepharose was dephosphorylated or phosphorylated by treatment with either phosphatase PP2c (400 ng, 2 mM $MgCl_2$, 32 °C, 60 min) or FLAG-CaMKKβ (50 ng, 2 mM $MgCl_2$, 200 μM ATP, 32 °C, 10 min), respectively. PP2c or CaMKKβ was removed by 5 × 1-mL washes (50 mM Tris • HCl, pH 7.4, 50 mM NaCl, 10% glycerol, 1 mM DTT) prior to AMPK elution with wash buffer + 20 mM glutathione. Human LKB1, MO25α, and STRADα cDNAs were generous gifts from Dr. Neal Birnberg (Mercury Therapeutics, Inc., Woburn, MA). MO25α was cloned into pcDNA4 Max to allow purification of the heterotrimer complex on Ni-nitrilotriacetate agarose (Qiagen) following triple transfection and expression in COS7 cells. Complex formation by all three subunits was confirmed by immunoblotting.

Mouse Skeletal Muscle AMPK α2 Immunoprecipitation. Mouse skeletal muscle was homogenized in lysis buffer [50 mM Tris • HCl, pH 7.5, 1 mM DTT, 1 mM EDTA, 1 mM EGTA, 10% (vol/vol) glycerol, 1% (vol/vol) Triton X-100, 50 mM NaF, 5 mM Na pyrophosphate] supplemented with protease inhibitor cocktail (Roche). AMPK was PEG 6K precipitated (2–6%) from cleared lysates, resuspended in lysis buffer, and incubated with protein A agarose beads (Sigma) coated with AMPK α2-specific antibody. Beads were washed thoroughly and boiled in SDS-PAGE sample buffer. Following SDS-PAGE/Coomassie staining, the AMPK β2 band was excised and subjected to tryptic digestion prior to peptide analysis by mass spectrometry.

Mass Spectrometry. N-Terminally Myristoylated β2 Peptide Sequencing. AMPK β2 immunoprecipitated from mouse skeletal muscle was digested from a SDS gel with trypsin (Promega) in 20 mM NH_4HCO_3 and the MS-compatible detergent Invitrisol (Invitrogen). Extracted peptides were dried under vacuum and resuspended in 20 μL 1.5% formic acid/25% acetonitrile (ACN). Nanochromatography was performed on a Dionex Ultimate 3000 at a flow rate of 500 nL/min using a homemade 25 cm × 75 μm column packed with Pepmap100 C18 (LC Packings). A 3–85% ACN gradient was required to resolve the highly hydrophobic myristoylated peptide. MS was performed on a QSTAR Pulsar i using a microionspray source (Applied Biosystems). Data were acquired using an automated program targeting singly charged ions between 950–1,000 atomic mass units.

Protein Mass Determination. Protein samples were methanol precipitated and resuspended in 20 μL 30% acetic acid. Proteins were resolved on a 2.1 × 75 mm Poroshell 300SB-C8 column (Agilent) with a 3–55% ACN gradient at 250 μL/min using a Dionex Ultimate 3000 LC. MS was performed on a QSTAR Pulsar i using a turboionspray source (Applied Biosystems).

AMPK α-Thr172 Phosphorylation/Dephosphorylation Assays. Phosphorylation assays: COS7 cell-expressed, PP2c-dephosphorylated AMPK was used unless stated. Purified AMPK (100 ng) was incubated with either 1.6 ng CaMKKβ (32 °C, 10 min) or 150 ng LKB1 heterotrimer (32 °C, 30 min) in the presence of 2 mM $MgCl_2$, 200 μM ATP, and AMP in the range 0–500 μM as indicated (final reaction volume 15 μL). Phosphorylation assays involving CaMKKβ were conducted with a final NaCl concentration of 120 mM unless stated, whereas phosphorylation assays involving LKB1 heterotrimer were conducted with a final NaCl concentration of 50 mM. Dephosphorylation assays: COS7 cell-expressed, CamKKβ-phosphorylated AMPK (100 ng) was incubated with 100 ng PP2c, 2 mM $MgCl_2 \pm 200$ μM AMP. For both assays, the final reaction volume was 15 μL, conditions were optimized to ensure phosphorylation/dephosphorylation rates remained linear with respect to time and protein concentration. Reactions were terminated by addition of 15 μL SDS-PAGE sample buffer, boiled and immunoblotted simultaneously for α-pThr172 and total α.

Immunoblotting. Samples were electrophoresed by 10% SDS-PAGE and transferred to Immobilon FL polyvinylidine-flouride membrane (Millipore). The membrane was blocked with 2% nonfat dry milk in phosphate-buffered saline + 0.1% Tween 20 (PBS-T) for 1 h at room temperature. To measure α-pThr172, membranes were simultaneously probed for 1 h at room temperature with a phosphospecific 1° antibody for α-pThr172 (1:10,000 dilution in PBS-T) labeled with the fluorescent dye IR680 (LI-COR Biosciences) and α1- or α2-specific 1° antibodies (1:5,000 dilution in PBS-T) fluorescently labeled with IR800. Relevant phosphospecific 1° antibodies (1:2,000 dilution in PBS-T) were used to measure β-pSer108 or α-pSer485, followed by incubation with anti-rabbit IgG 2° antibody fluorescently labeled with IR680. Immunoreactive bands were visualized on an Odyssey membrane imaging system (LI-COR Biosciences) and densitometry analyses performed using integrated software.

AMPK Activity Assay. AMPK complexes were purified by glutathione-Sepharose pull down and washed extensively with assay buffer (50 mM Hepes; pH 7.4, 1 mM DTT, 0.02% Brij-35). Activity was determined on beads by phosphorylation of the SAMS peptide using 100 μM SAMS, 200 μM [γ-^{32}P] ATP, 5 mM $MgCl_2 \pm 200$ μM AMP in a standard 25 μL volume assay at 30 °C. Reactions were terminated after 10 min by spotting 15 μL onto P81 phosphocellulose paper (Whatman) and washing in 1% phosphoric acid. Radioactivity was quantified by scintillation counting. For the linked CaMKKβ-mediated α-Thr172 phosphorylation/AMPK activity assay, 640 ng purified COS7-cell-ex-

pressed AMPK was incubated with 8 ng CaMKKβ (32 °C, 20 min) in the presence of 2 mM $MgCl_2$, 200 ± 200 μM AMP (final reaction volume 20 μL). 2 μl of the reaction was removed and immediately assayed for AMPK activity as described above (300 μM [γ-^{32}P] ATP), with final AMP concentration adjusted to 200 μM to account for allosteric effects.

Liposome Preparation and Partitioning Assay. Small unilamellar vesicles were prepared from chloroform dissolved mixtures of palmitoyl-oleoyl phosphatidylserine and palmitoyl-oleoyl phosphatidylcholine by hydrating a dried lipid film with 50 mM Tris • HCl, pH 7.4, 150 mM NaCl at 25 °C on a rotating platform. The lipid suspension was sonicated for 2 × 10 min in a bath sonicator. After annealing for 30 min, liposomes were sedimented at 20,000 × *g* for 30 min, resuspended in an equal volume of hydration buffer and used within 3 d of preparation. One-hundred nanograms of purified AMPK was incubated with liposomes (5 μL) ± 500 μM AMP (final NaCl concentration 150 mM, final volume 20 μL) for 2 min at 25 °C. Liposomes were sedimented at 20,000 × *g*, 15 min, 25 °C, and α1 content of soluble and pelleted membrane fractions was detected by immunoblotting.

Fluorescence Microscopy. The expression vector pEGFP-C1 was used to construct a plasmid encoding N-terminal GFP-tagged α1-subunit. COS7 cells in 3.5 cm culture plates were cotransfected with GFP-α1, γ1 and WT or G2A mutant β1 (100 ng total DNA per plate) and incubated for 16 h, after which medium was replaced with fresh high glucose (5 mM) DMEM for 2 h. Nutrient stress was induced by replacing medium with no glucose DMEM for 60 min. Plasma membrane permeabilization was performed by washing cells with ice-cold PBS then incubating with PBS containing 0.01% (wt/vol) digitonin for 2 min, before washing again with PBS. Cells were visualized on a Zeiss Axiovert 25 microscope fitted with a UV lamp and images were taken with a Zeiss AxioCam digital camera.

Statistical Analysis. Data are presented as mean values ± SEM of at least three independent experiments. The unpaired two-tailed Student's *t* test was used for all comparisons.

SI note 1. We attempted to use inside-out (IO) vesicles derived from rabbit erythrocytes (following the protocol of Steck and Kant, ref. 4) as an alternative membrane model to demonstrate AMP-mediated myristoyl switching by AMPK. In some experiments, we observed an AMP-induced increase in membrane partitioning from a basal level of 36% total AMPK to 71%. However, the results were quite variable between different IO vesicle preparations and data have not been included here.

SI note 2. In the AMPK α2 kinase domain crystal structure (PDB ID code 2H6D), the opening to a pocket corresponding to the Abl myristoyl binding site is obstructed by the side chain of Arg110 located on a loop between helices αD and αE, and also by the side chain of Leu208 positioned further into the cavity. In addition, the AMPK α2 structure varies from the PKA structure in the region corresponding to the PKA myristoyl binding site due to flattening of the kinase domain C-terminal α-helix (α2 Pro273-Phe279). A similar distortion is observed in the crystal structure of the *Schizosaccharomyces pombe* Snf1 kinase domain plus autoregulatory sequence (5) (PDB ID code 3H4J). However, one interpretation is that the conformation adopted reflects the absence of myristoyl binding.

SI note 3. LKB1/MO25α/STRADα was expressed in COS7 cells with GST-tagged LKB1 and His6-tagged MO25α. It should be noted that commercial Sf21-expressed LKB1 construct (Millipore) yielded <1.3-fold maximal AMP-activation. This construct has GST-tags associated with both LKB1 and MO25α subunits.

1. Iseli TJ, et al. (2008) AMP-activated protein kinase subunit interactions: beta1:gamma1 association requires beta1 Thr-263 and Tyr-267. *J Biol Chem* 283:4799–4807.
2. Warden SM, et al. (2001) Post-translational modifications of the beta-1 subunit of AMP-activated protein kinase affect enzyme activity and cellular localization. *Biochem J* 354:275–283.
3. Duronio RJ, et al. (1990) Protein N-myristoylation in *Escherichia coli*: Reconstitution of a eukaryotic protein modification in bacteria. *Proc Natl Acad Sci USA* 87:1506–1510.
4. Steck TL, Kant JA (1974) Preparation of impermeable ghosts and inside-out vesicles from human erythrocyte membranes. *Method Enzymol* 31:172–180.
5. Chen L, et al. (2009) Structural insight into the autoinhibition mechanism of AMP-activated protein kinase. *Nature* 459:1146–1149.

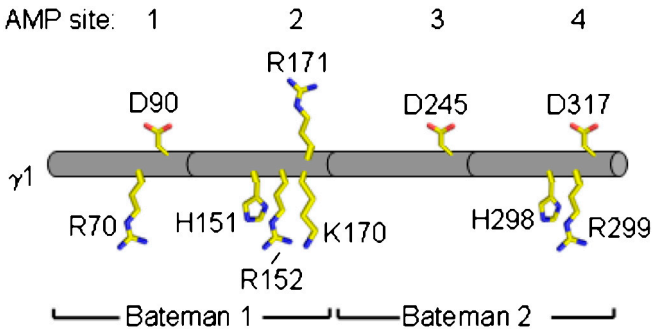

Fig. S1. Distribution of basic residues involved in nucleotide binding to γ1. Conserved Asp residues that hydrogen bond with AMP ribose group hydroxyls and corresponding nucleotide sites in γ are indicated above. Basic residues that hydrogen bond to nucleotide phosphates are shown below. Residue numbers based on human sequence.

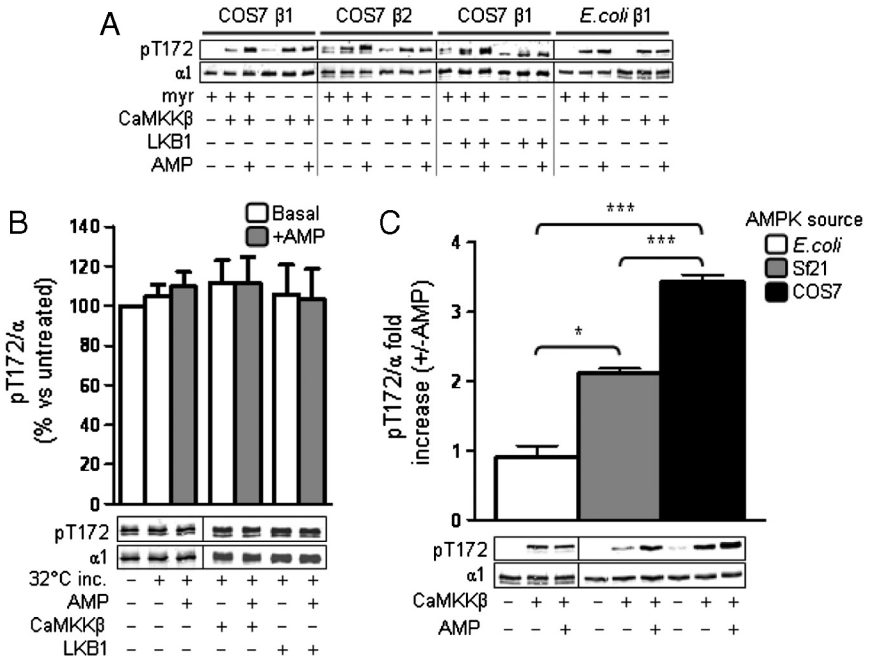

Fig. S2. The β-subunit myristoylation regulates AMP-activated phosphorylation of α-Thr172. All values are presented as mean ± SEM, $n = 3–7$. Immunoblots shown are single representative experiments, vertical lines indicate separate gels. (*A*) Representative immunoblots from AMP-activated Thr172 phosphorylation assays detailed in Fig. 1*A*. Source of AMPK and the β isoform within each α1βγ1 complex are indicated above. The β-subunit myristoylation state and upstream kinase used in the phosphorylation assay are indicated below. Myristoylated AMPK was produced in *E. coli* by coexpression with N-myristoyl transferase. (*B*) Protein preparations lack AMP-sensitive phosphatase activity. Mock phosphorylation assays were conducted as described but omitting ATP, using phosphorylated AMPK incubated (32 °C inc.) alone or with either CamKKβ or LKB1 ± AMP (500 μM). pThr172 and total α were detected by immunoblot and compared to a nonincubated control. Immunoblot shown is a single representative experiment. (*C*) AMP stimulation of Thr172 phosphorylation varies with source of recombinant AMPK. Dephosphorylated AMPK, purified from Sf21 or COS7 cells, or AMPK purified from *E. coli* was phosphorylated by CaMKKβ ± AMP (500 μM). $*P < 0.02$ and $***P < 0.001$.

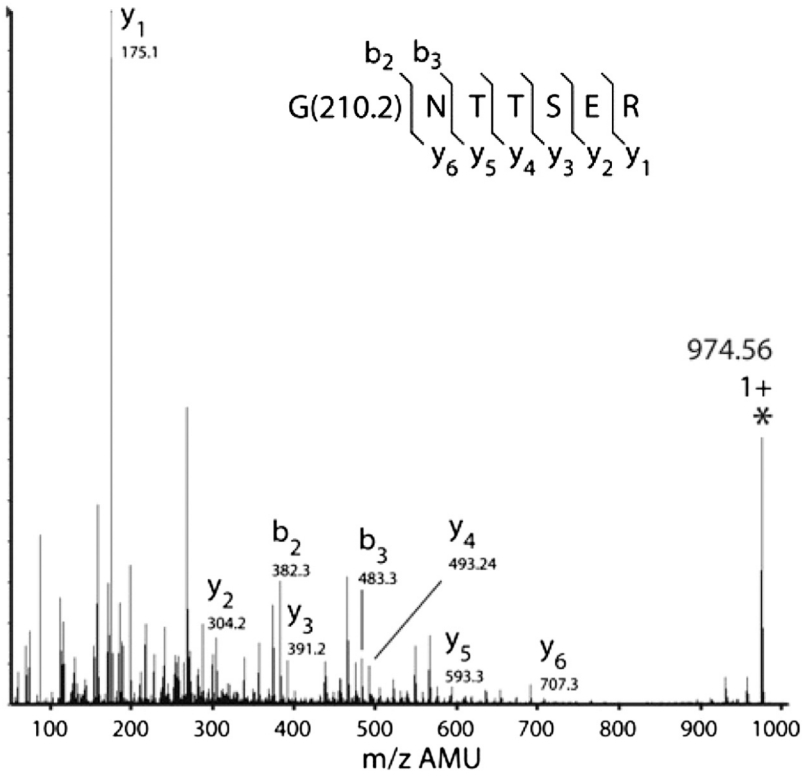

Fig. S3. The β2-subunit of mouse skeletal muscle AMPK is modified by N-terminal myristoylation. Mouse skeletal muscle α2-AMPK was isolated by immunoprecipitation and subunits resolved by SDS-PAGE. The β2 band was excised and subjected to tryptic digest and MS/MS peptide analysis. Masses of the parent ion and the b and y series ions provide unequivocal evidence that β2-Gly2 is myristoylated.

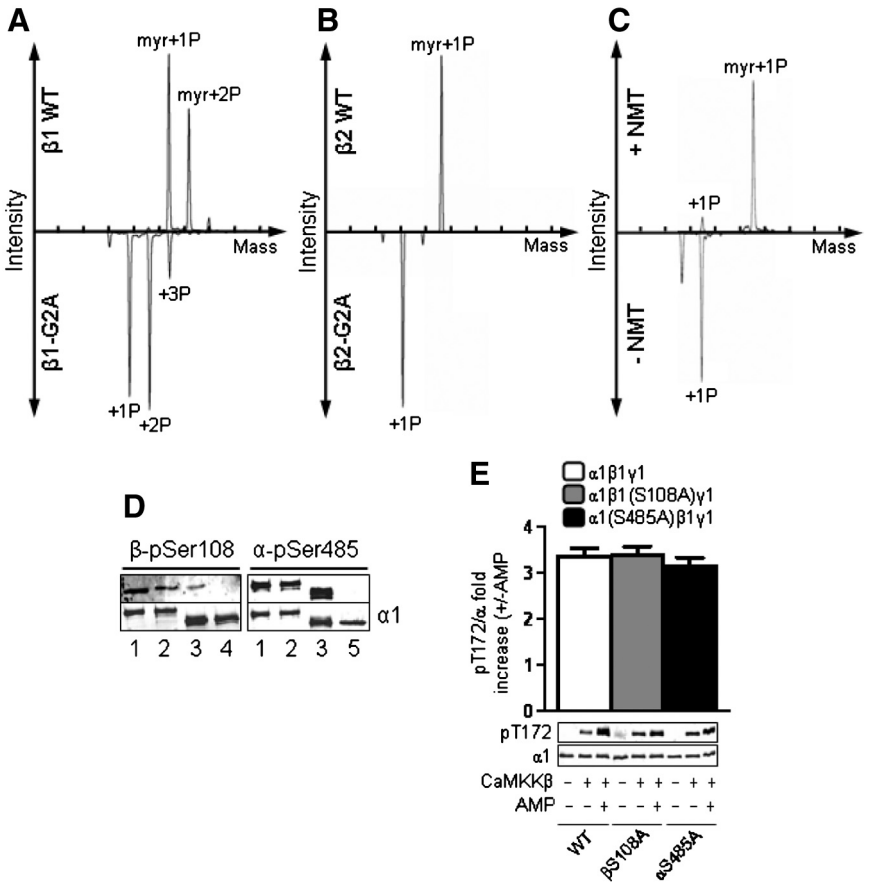

Fig. S4. Recombinant protein subunit modifications. Deconvoluted TOF spectra of (*A*) β1-subunit and (*B*) β2-subunit isoforms from PP2c-dephosphorylated, purified AMPK expressed in COS7 cells (upper, β WT; lower, β-G2A), and (*C*) AMPK expressed in *E. coli*, either with N-myristoyl transferase (NMT) (*Upper*) or without NMT (*Lower*). The *x*-axis graduations represent 100 atomic mass units, observed masses for each species are listed in Table S2. (*D*) Identification of phosphorylation sites in *E.-coli*-expressed AMPK. Purified AMPK samples from various sources were immunoblotted for β1-pSer108 (*Upper Left*) or α1-pSer485 (*Upper Right*). Lanes: 1, *E.-coli*-expressed myristoylated α1β1γ1 (MBP-tagged α1); 2, *E.-coli*-expressed nonmyristoylated α1β1γ1; 3, COS7 cell-expressed α1β1γ1; 4, COS7 cell-expressed α1β1(S108A)γ1; 5, COS7 cell-expressed α1(S485A)β1γ1. (*E*) Mutation of autophosphorylation sites β1-Ser108 or α1-Ser485 does not alter AMP stimulation of Thr172 phosphorylation. $n = 3$, all values are presented as mean ± SEM. Immunoblot shown is a single representative experiment.

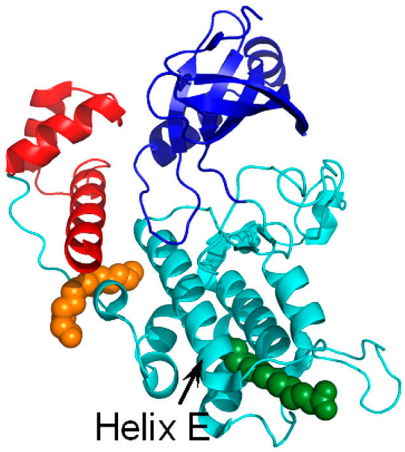

Fig. S5. Protein kinase domain-associated myristoyl binding sites. Shown is the crystal structure of the *Schizosaccharomyces pombe* Snf1 kinase domain [PDB ID code 3H4J (1) small lobe, dark blue; large lobe, cyan, autoregulatory sequence, red) and superimposition of myristoyl groups from PKA (orange) or Abl (green) within the AMPK catalytic core. See also SI Note 2.

1 Chen L, et al. (2009) Structural insight into the autoinhibition mechanism of AMP-activated protein kinase. *Nature* 459:1146–1149.

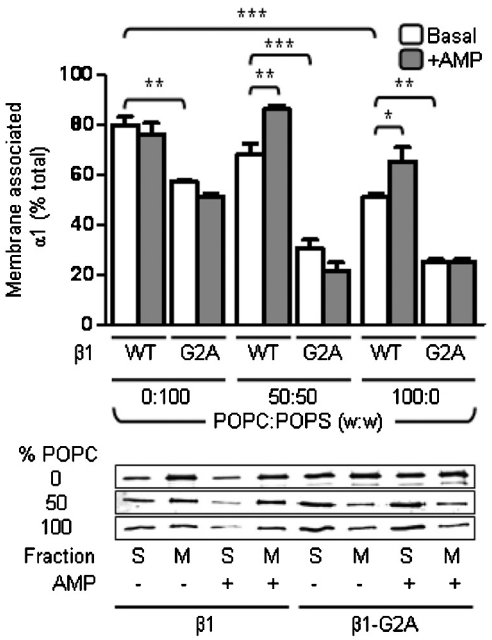

Fig. S6. Effect of membrane surface charge on AMP-regulated AMPK membrane association. Experiments were conducted as described for Fig. 4*A*, using liposomes prepared from varying POPC:POPS ratios as indicated. $n = 3–7$, $^{*}P < 0.05$, $^{**}P < 0.01$, and $^{***}P < 0.001$. All values are presented as mean ± SEM. Immunoblots shown are of single representative experiments for each liposome type.

Table S1. Summary of expression plasmids

Plasmid	Protein* (mutation)	Oligonucleotides (sense)	Source
Bacterial expression			
pST39	MBP-TEV-α1β1γ1	—	This study
pBB131	N-myristoyl transferase	—	(1)
Baculovirus expression			
pFastBac1:	FLAG-TEV-CaMKKβ	—	(2)
	GST-TEV-mouse PP2c	—	This study
Mammalian cell expression		—	
pDEST27	GST-α1	—	(2)
pcDNA3.1	GST-α2	—	This study
	β1	—	This study
	β1(G2A)	GACTCGAGATCATGGCAAATACCAGCAGTG	This study
	β1(S108A)	CCCCTCACCAGAGCCCACAATAACTTTGTAGC	This study
	β1(D224A)	GGGGATTTCCTGTGCTCCAGCTTTGCTTCC	This study
	β2	—	This study
	β2(G2A)	CTAGACTCGAGGCCATGGCAAACACCACCAGC	This study
pMT2	HA-γ1	—	(3)
	HA-γ1(D90A)	CTGACCATCACTGCTTTCATCAATATCCTG	This study
	HA-γ1(D245A)	TACTCCAAGTTTGCTGTTATCAATCTGGCA	This study
	HA-γ1(R299G)	GGAAGCAGAGGTTCACGGACTTGTAGTGGTGG	This study
	HA-γ1(D317A)	GTATCACTGTCTGCCATCCTGCAGGCCCTG	This study
pEBG	GST-rat α1(S485A)	CCACAGAGATCGGGAGCCATCAGCAACTATCG	This study
	GST-LKB1	—	This study
pcDNA4 Max	His-MO25α	—	This study
pCMV	FLAG-STRADα	—	This study
pEGFP-C1	GFP-α1		This study

Sequences are oligonucleotides used to generate mutations (underlined). TEV, Tobacco Etch Virus protease.
*Human sequence unless stated.

1 Duronio RJ, et al. (1990) Protein N-myristoylation in *Escherichia coli*: Reconstitution of a eukaryotic protein modification in bacteria. *Proc Natl Acad Sci USA* 87:1506–1510.
2 Iseli TJ, et al. (2008) AMP-activated protein kinase subunit interactions: beta1:gamma1 association requires beta1 Thr-263 and Tyr-267. *J Biol Chem* 283:4799–4807.
3 Dyck JR, et al. (1996) Regulation of 5'-AMP-activated protein kinase activity by the noncatalytic beta and gamma subunits. *J Biol Chem* 271:17798–17803.

Table S2. TOF mass spectrometry data

Source	Subunit	Modification	ΔM_r,* Da	M_r, Da	
				M_r(calc)	M_r(obs)
COS7	β1	—	—	30,251	—
		+myr +1P	+290	30,541	30,542
		+myr +2P	+370	30,621	30,622
		+myr +3P	+450	30,701	30,702
	β1-G2A	—	+56†	30,307	30,306
		+1P	+136	30,387	30,386
		+2P	+216	30,467	30,466
		+3P	+296	30,547	30,546
	β2	—	—	30,171	—
		+myr +1P	+290	30,461	30,462
	β2-G2A	—	+56†	30227	—
		+1P	+136	30,307	30,307
E. coli	β1	—	—	30,251	—
		+1P	+80	30,331	30,331
		+myr +1P	+290	30,541	30,541

P, phosphate group; myr, myristoyl group.
*Relative to unmodified WT mass.
†net ΔM_r: G2A mutation $= +14$ Da, Ala acetylation $= +42$ Da.